Alloying barbituric and thiobarbituric acids: from solid solutions to a highly stable *keto* co-crystal form.

O. Shemchuk,[a] D. Braga,[a] and F. Grepioni[a,*]

[a] Dipartimento di Chimica "G. Ciamician", Universiy of Bologna, Via Selmi, 2 – 40126 Bologna – Italy.

Electronic Supplementary Information

Solution Synthesis. All reactants and reagents were purchased from Sigma-Aldrich and used without further purification. Reagent grade solvents and bi-distilled water were used.

All the solid solutions of BA and TBA acids with general formula BA_xTBA_{1-x} were obtained by dissolution of the *x* and *1-x* quantities of the starting materials (see ESI-Table 1) in 20 mL of boiling EtOH; the solution was left to evaporate at room temperature.

ESI-Table 1. Quantities of reagents employed in the crystallizations from solution.

BA:TBA ratio	BA, mg (mmol)	TBA, mg (mmol)
$BA_{0.2}TBA_{0.8}$	25.6 (0.2 mmol)	115.3 (0.8 mmol)
$BA_{0.3}TBA_{0.7}$	38.4 (0.3 mmol)	100.9 (0.7 mmol)
$BA_{0.4}TBA_{0.6}$	51.2 (0.4 mmol)	86.5 (0.6 mmol)
$BA_{0.5}TBA_{0.5}$	64.0 (0.5 mmol)	72.1 (0.5 mmol)
$BA_{0.6}TBA_{0.4}$	76.8 (0.6 mmol)	57.7 (0.4 mmol)
$BA_{0.7}TBA_{0.3}$	89.7 (0.7 mmol)	43.2 (0.3 mmol)
$BA_{0.8}TBA_{0.2}$	102.5 (0.8 mmol)	28.8 (0.2 mmol)

Solid State Synthesis. $BA_{0.5}TBA_{0.5}$ was also obtained by kneading either thiobarbituric acid form I (*keto*-form) with ethanol, or thiobarbituric acid form IV (*keto-enol* form) with acetonitrile. 1 mmol of BA and TBA were kneaded for 20 minutes in a Retsch MM200 ball miller, operated at a frequency of 20 Hz, in the presence of a few drops of the corresponding solvent.

Crystal structure determination. Single-crystal data for BA_xTBA_{1-x} (x≥0.5) were collected at RT on an Oxford X'Calibur S CCD diffractometer equipped with a graphite monochromator (Mo-Kα radiation, λ = 0.71073 Å). Data collection and refinement details are listed in Table ESI-S2. The program SHELX97[ESI-1a] was used for structure solution and refinement on F^2. The program Platon[ESI-1b] was used to calculate intermolecular interactions. Schakal99[ESI-1c] was used for molecular graphics. In BA_xTBA_{1-x} (x≥0.5) the S and O atoms (indicated by an arrow in Figure ESI-1) of each independent molecule were treated as disordered over two positions: the occupancy factor was first refined by keeping the isotropic thermal parameters fixed, than the occupancy factor was fixed and both oxygen and sulphur atoms were refined anisotropically. All non-hydrogen atoms were refined anisotropically. H_{CH} and H_{NH} atoms were added in calculated positions and refined riding on their respective carbon or nitrogen atoms.

Crystal data can be obtained free of charge *via* www.ccdc.cam.ac.uk/conts/retrieving.html (or from the Cambridge Crystallographic Data Centre, 12 Union Road, Cambridge CB21EZ, UK; fax: (+44)1223-336-033; or e-mail: deposit@ccdc.cam.ac.uk). CCDC numbers 1498572 ($BA_{0.5}TBA_{0.5}$), 149574 ($BA_{0.6}TBA_{0.4}$) and 149573 ($BA_{0.7}TBA_{0.3}$).

ESI-1 (a) G. M. Sheldrick, G. M. SHELX97, Program for Crystal Structure Determination; University of Göttingen: Göttingen, Germany, 1997; (b) A. L. Spek, Acta Cryst. 2009, D65, 148-155; (c) E. Keller, SCHAKAL99, Graphical Representation of Molecular Models; University of Freiburg: Freiburg, Germany, 1999.

ESI-Table 1. Single crystal data for the B_xTBA_{1-x} solid solutions with x ≥ 0.5, and comparison with data for BA form II at room temperature[b] and TBA form I [THBARB] at room temperature.

	TBA form I (THBARB)	$BA_{0.5}TBA_{0.5}$	$BA_{0.6}TBA_{0.4}$	$BA_{0.7}TBA_{0.3}$	$BA_{0.8}TBA_{0.2}$[a]	BA form II RT[b]
Formula	$C_4H_4N_2O_2S$	$C_4H_4N_2O_{2.5}S_{0.5}$	$C_4H_4N_2O_{2.6}S_{0.4}$	$C_4H_4N_2O_{2.7}S_{0.3}$	$C_4H_4N_2O_{2.8}S_{0.2}$	$C_4H_4N_2O_3$
fw	144.15	136.12	134.52	132.91	131.31	128.09
Cryst. System	monoclinic	monoclinic	monoclinic	monoclinic	monoclinic	monoclinic
space group	$P2_1/c$	$P2_1/c$	$P2_1/c$	$P2_1/c$	$P2_1/c$	$P2_1/c$
Z, Z'	8, 2	8, 2	8, 2	8, 2	8, 2	8, 2
a (Å)	8.450(10)	8.533(1)	8.4662(13)	8.4569(9)	8.321(7)	8.199
b (Å)	13.140(20)	13.0141(10)	12.9681(12)	12.9400(10)	12.797(6)	12.613
c (Å)	10.420(10)	9.6918(12)	9.6819(11)	9.5593(9)	9.698(6)	9.823
α (deg)	90.00	90.0	90.0	90.0	90.0	90.00
β (deg)	92.70	92.131	92.490(14)	92.626(10)	93.70(6)	95.7
γ (deg)	90.00	90.0	90.0	90.0	90.0	90.00
V (Å³)	1155.679	1075.5(2)	1062.0(2)	1045.00(17)	1030.5(12)	1010.8
D_{calc} (g/cm³)	-	1.681	1.683	1.690	-	-
μ (mm⁻¹)	-	0.324	0.294	0.256	-	-
Measd reflns	-	4693	4603	4818	-	-
Indep reflns	-	2458	2431	2417	-	-
R1[on F_0^2, I>2σ(I)]	-	0.0856	0.1059	0.0743	-	-
wR2 (all data)	-	0.1552	0.2839	0.1604	-	-

[a] Unfortunately, despite many attempts at growing good quality single crystals of $BA_{0.8}TBA_{0.2}$, the quality of the best data set collected still does not reach the standard required for data deposition; however, the space group was ascertained with confidence, the sulphur contribution was evidenced and the cell volume was found to fit well within the trend from BA form II (room temperature data) to TBA form I (see below).
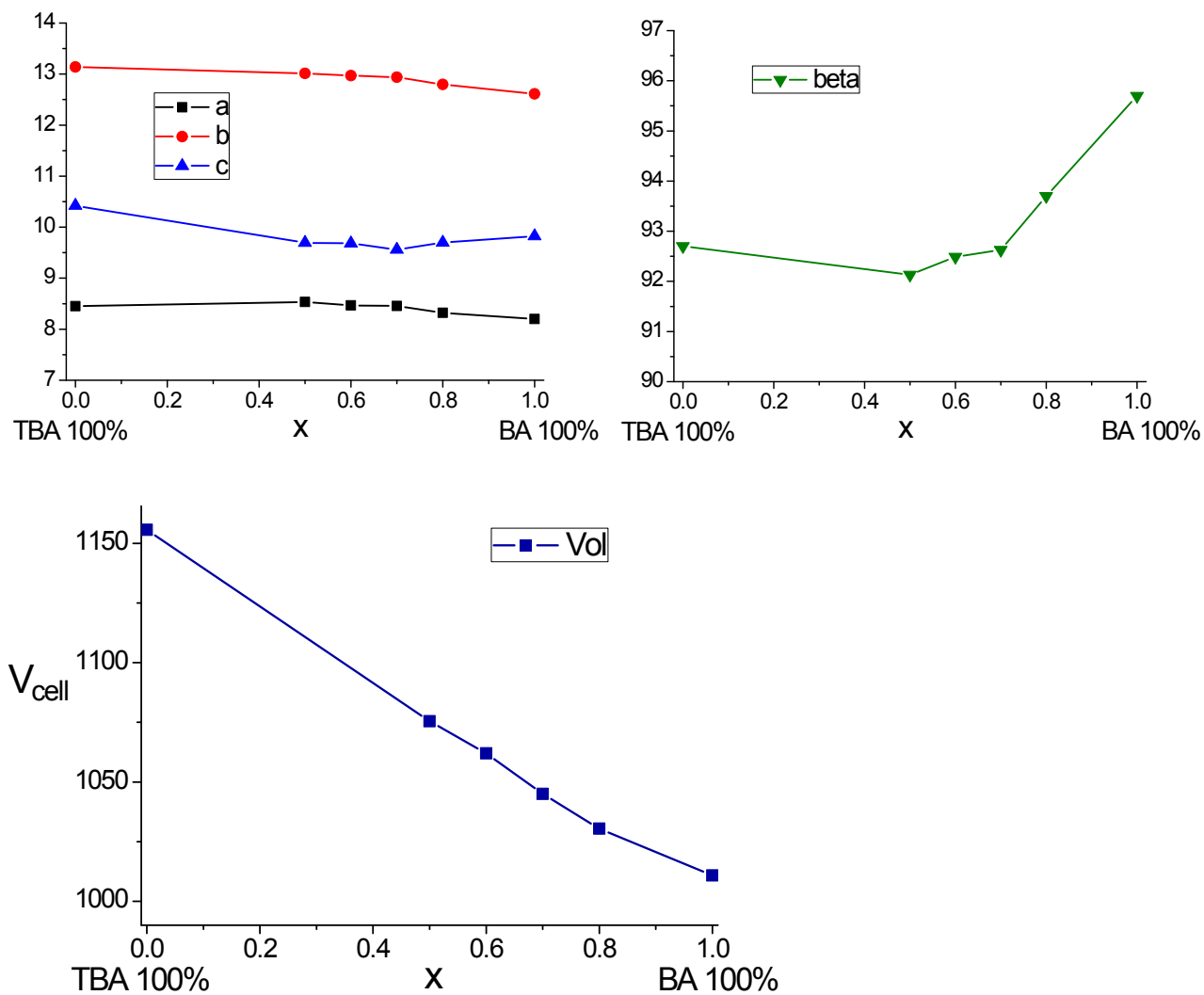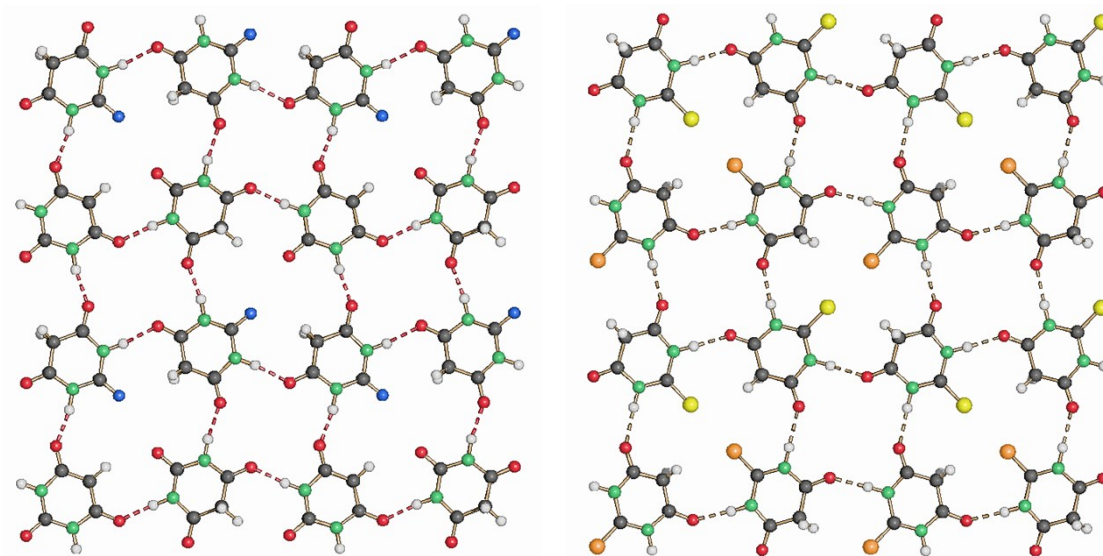
[b] See ref. 12b in the main article.

Figure ESI-1. Cell parameters variation (single crystals, *room temperature data*) on passing from TBA form I to BA Form II: cell axes (top left), monoclinic β angle (top right) and cell volume (bottom).
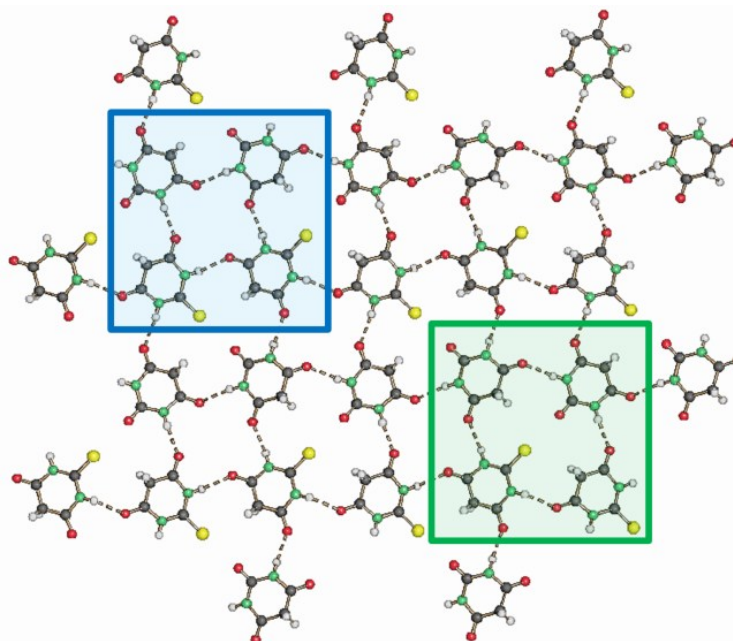
Figure ESI-2. The hydrogen bonding pattern observed in BA form II (top left, BARBAC02, O atoms of independent molecules shown in red and blue) and in TBA form I (top right, THBARB, S atoms of independent molecules shown in yellow and orange) is also maintained in the solid solutions; here the packing for the $BA_{0.5}TBA_{0.5}$ co-crystal is shown (bottom), with the two large hydrogen bonded rings forming 2D parallel planes perpendicular to the crystallographic *ac*-plane.

X-ray powder diffraction. Room temperature X-ray powder diffraction (XRPD) patterns were collected on a PANalytical X'Pert PRO automated diffractometer equipped with a X'celerator detector in the 2θ range 3–50° (step size 0.0334, time/step 30.480 s, VxA 40x40). Data analyses were carried out using the Panalytical X'pert Highscore Plus program. The identity between the bulk material obtained via olution and solid-state processes was verified by comparing calculated and observed powder diffraction patterns. The program Mercury[ESI-2a] was used for simulation of X-ray powder patterns on the basis of single crystal data, while the program PowderCell[ESI-2b] was used to simulate a powder pattern on the basis of cell parameters – thus to identify the angular position of relevant peaks – for $BA_{0.8}TBA_{0.2}$ and for BA form II at room temperature, for which only single crystal cell parameters were available.

References

ESI-2 (a) C. F. Macrae, I. J. Bruno, J. A. Chisholm, P. R. Edgington, P. McCabe, E. Pidcock, L. Rodriguez-Monge, R. Taylor, J. van de Streek and P. A. Wood, *J. Appl. Crystallogr.*, 2008, **41**, 466; (b) PowderCell 2.0, W. Kraus and G. Nolze (BAM Berlin) © subgroups derived by Ulrich Müller (Gh Kassel).
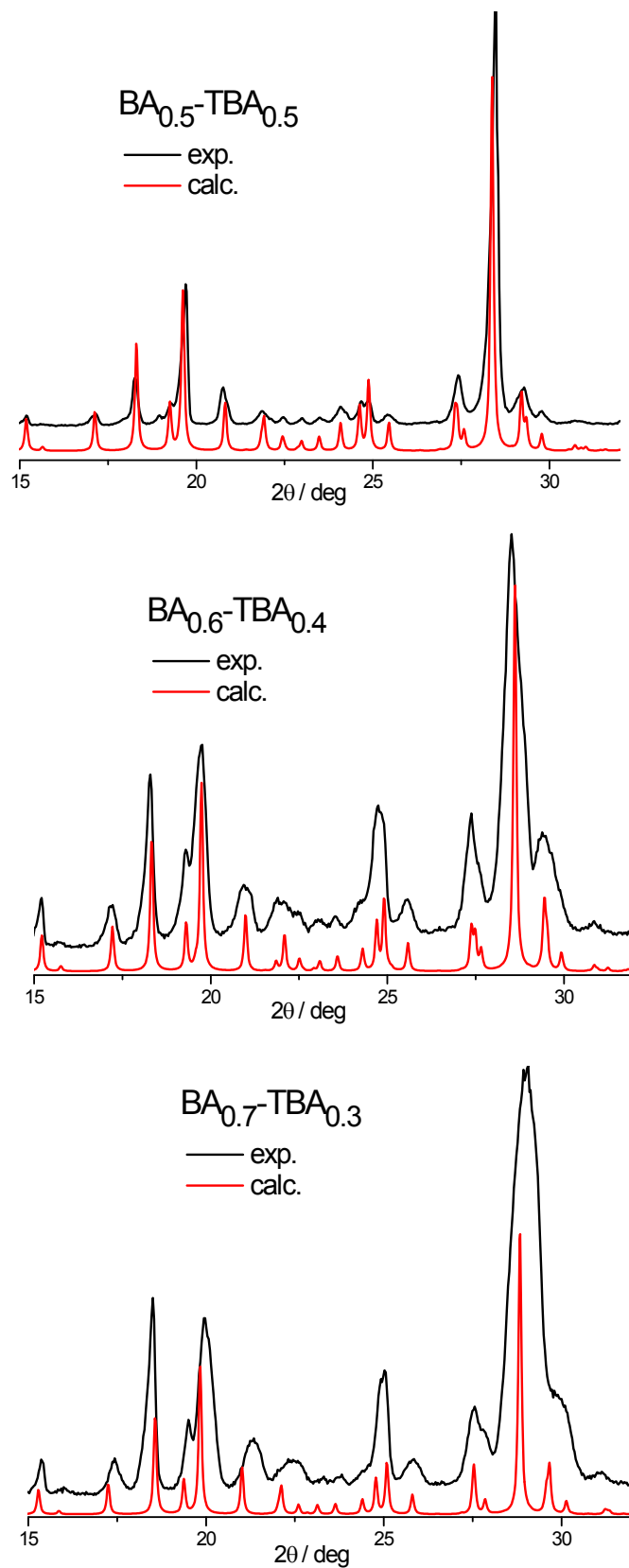
Figure ESI-1. Comparison of experimental (crystallizations from solution) and simulated patterns (on the basis of single crystal data) for $BA_{0.5}TBA_{0.5}$, $BA_{0.6}TBA_{0.4}$ and $BA_{0.7}TBA_{0.3}$.
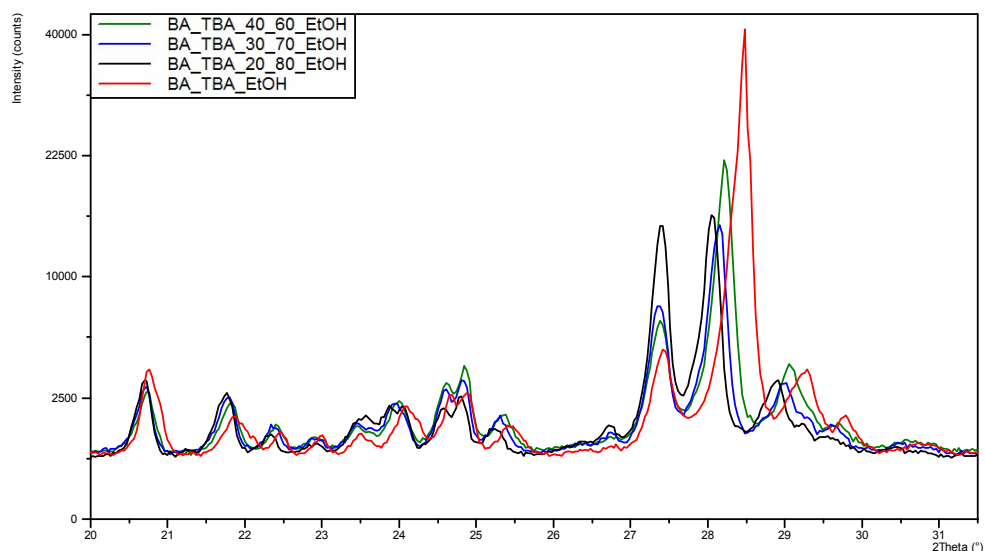
Fig. ESI-2. Experimental XRPD patterns for BA_xTBA_{1-x} solid solutions with $x \leq 0.5$: expanded section showing a general shift (analogous to what observed for the solid solutions with $x > 0.5$) of the peaks towards *lower* angles, on increasing the percentage of TBA, with respect to the $BA_{0.5}TBA_{0.5}$ co-crystal (red line).
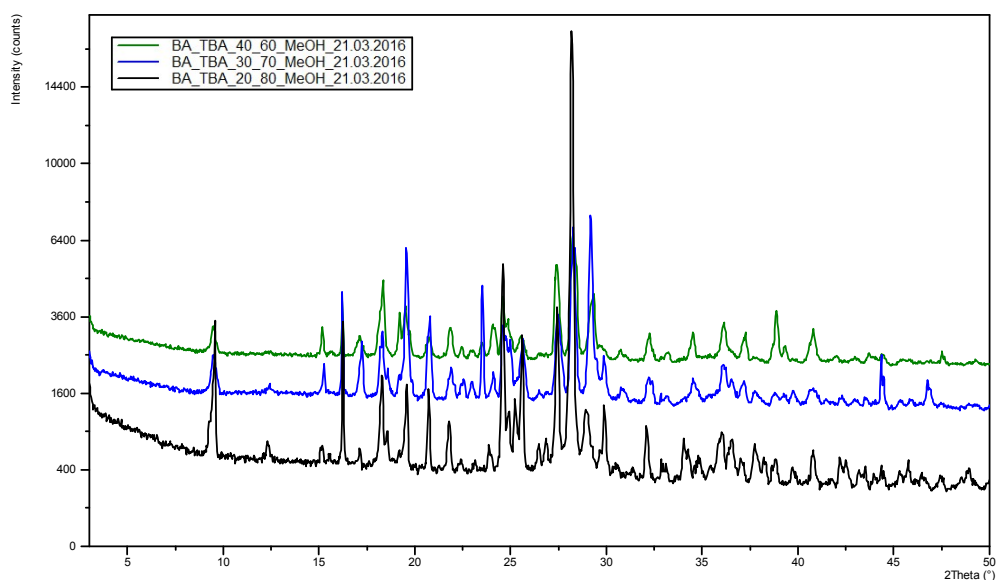
Figure ESI-3. Comparison between the XRPD pattern measured on the products obtained by crystallizing from MeOH BA form II and THBARB form I in 40:60 (top, green line), 30:70 (middle, blue line) and 20:80 (bottom, black line) molar ratios: $BA_{0.5}TBA_{0.5}$ is formed in all cases, together with unreacted TBA.
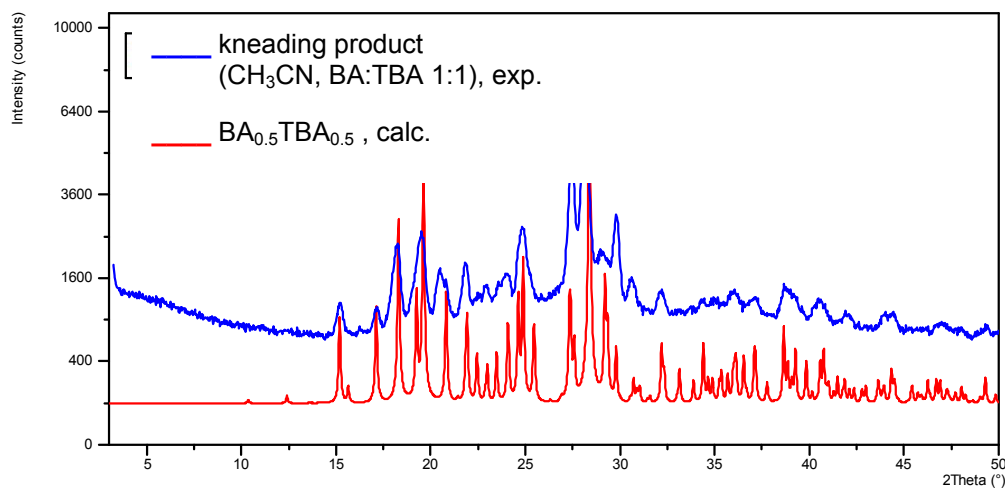
Figure ESI-4. Comparison between the XRPD pattern measured on the product obtained by kneading BA form II and THBARB form I in 1:1 molar ratio in the presence of a few drops of CH_3CN and (top, blue line) and the simulated pattern pattern (on the basis of single crystal data) for $BA_{0.5}TBA_{0.5}$.
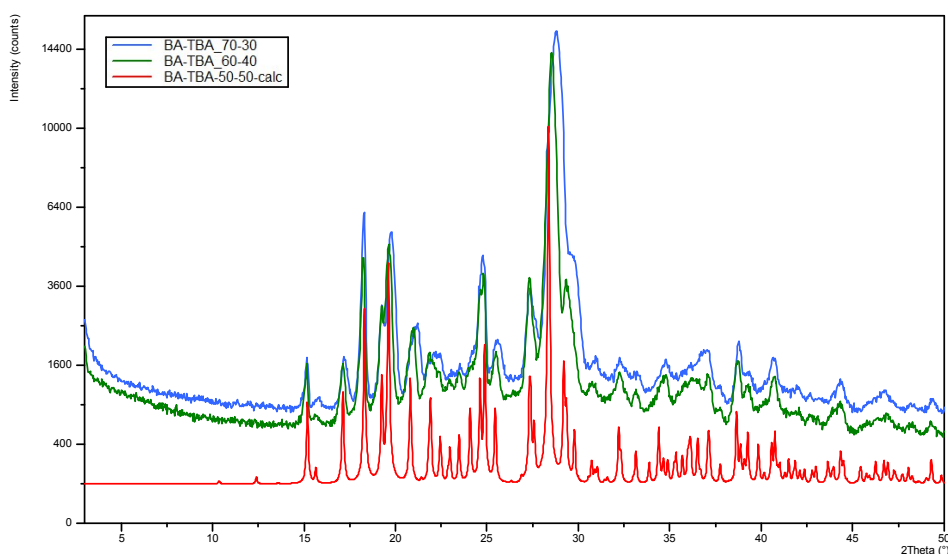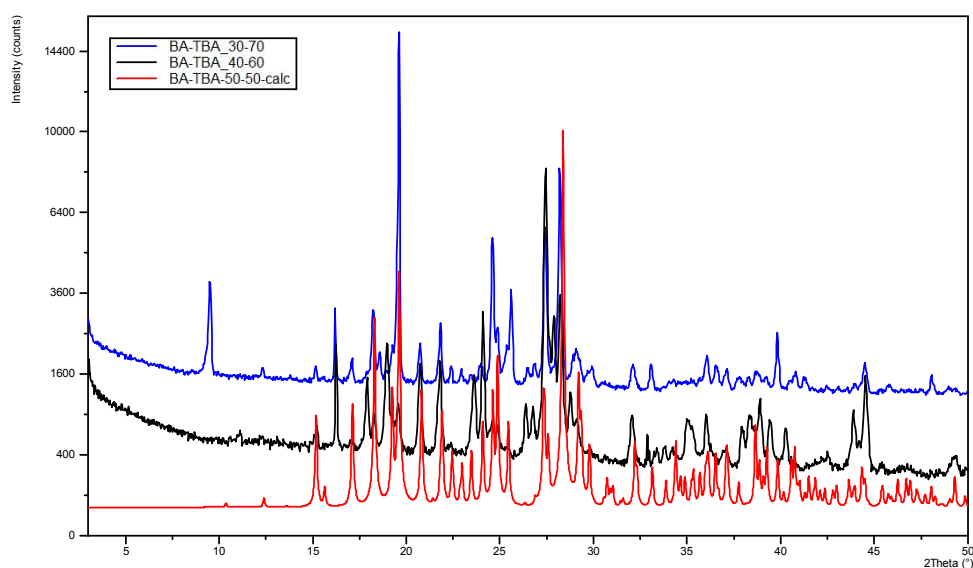

Figure ESI-5. Comparison between the XRPD experimental patterns measured after 3 months of standing in open air at ambient conditions on $BA_{0.7}TBA_{0.3}$ (blue line) and $BA_{0.7}TBA_{0.3}$ (green line) and the calculated pattern for $BA_{0.5}TBA_{0.5}$: the solid solutions are still unchanged.

Figure ESI-6. Comparison between the XRPD experimental patterns measured after 1 month of standing in open air at ambient conditions on $BA_{0.3}TBA_{0.7}$ (blue line) and $BA_{0.4}TBA_{0.6}$ (black line) and the calculated pattern for $BA_{0.5}TBA_{0.5}$: the solid solutions have converted into the co-crystal $BA_{0.5}TBA_{0.5}$ plus an excess of TBA form I.

Hot Stage Microscopy (HSM). HSM measurements were carried out using a Linkam TMS94 device connected to a Linkam LTS350 platinum plate. Images were collected with the imaging software Cell, from a Visicam 5.0 stereoscope. Images (100x) were taken with an Olympus optical microscope.
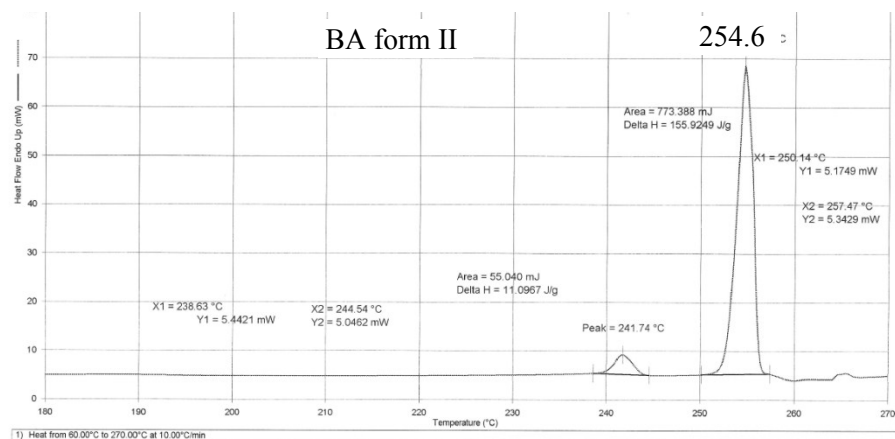
Differential Scanning Calorimetry (DSC)

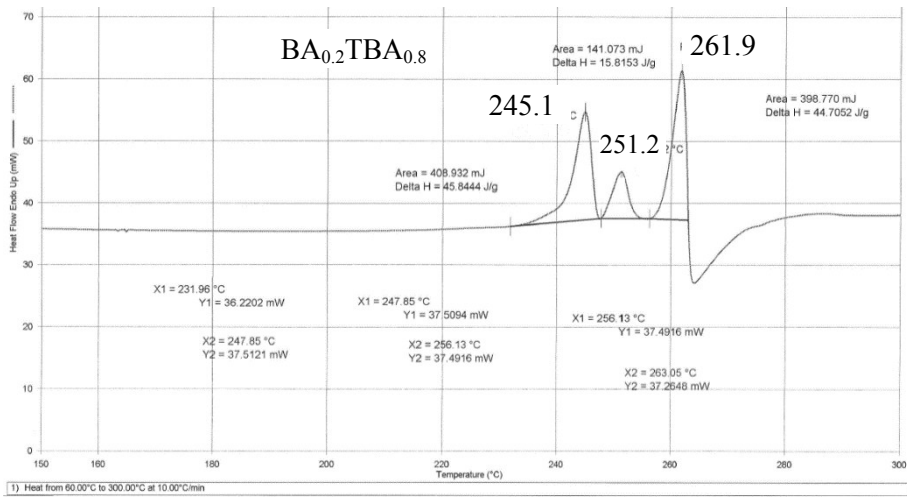DSC measurements were performed with a Perkin–Elmer Diamond. The samples (3-10 mg) were placed in open aluminum pans, and the heating was carried out at 10 °C min^{-1} in N$_2$ atmosphere.

Peak temperatures (°C) are indicated in all DSC heating traces shown in the following.
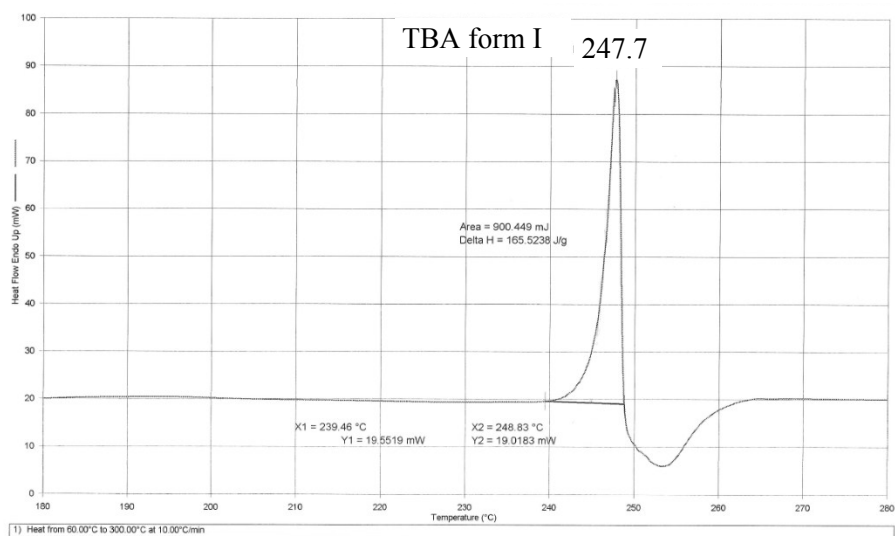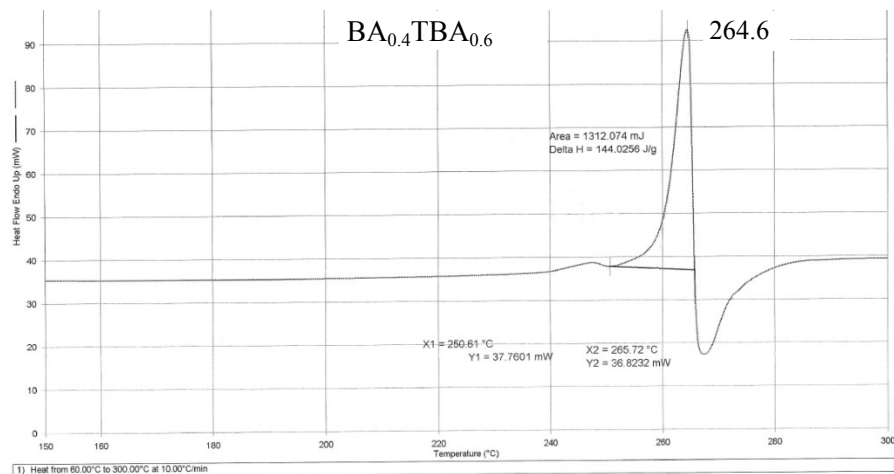

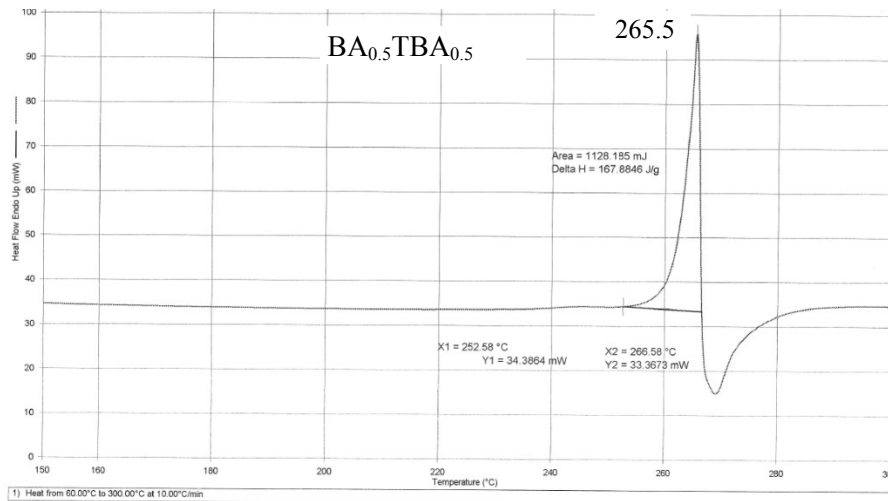DSC trace of TBA form I

DSC trace of BA form II

DSC trace of the product of crystallization of BA form II and TBA form I in 20:80 stoichiometric ratio.
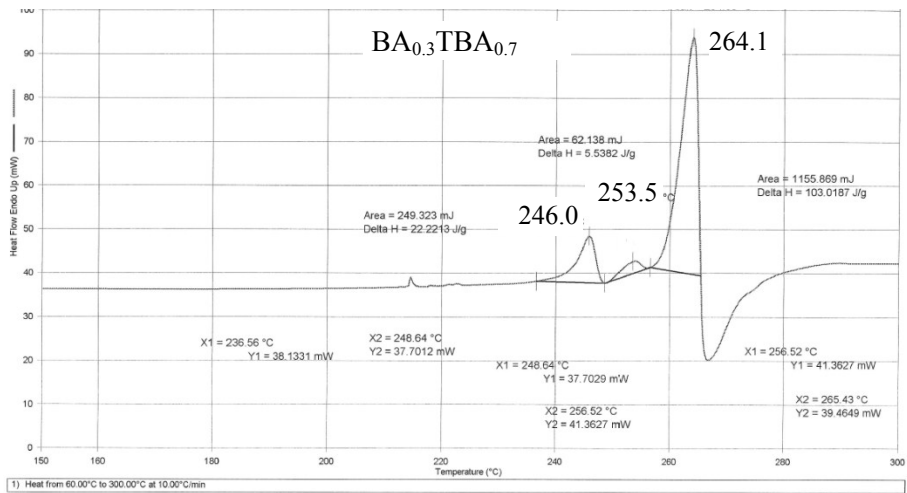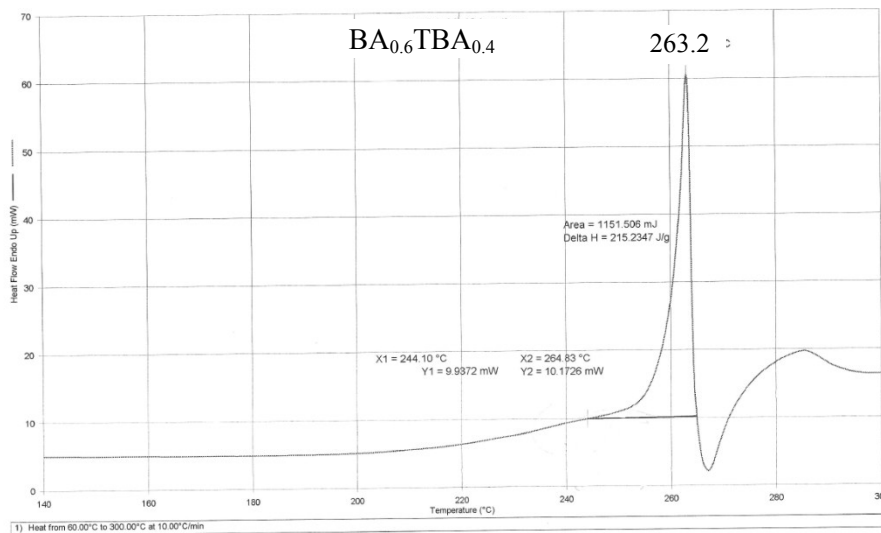

DSC trace of the product of crystallization of BA form II and TBA form I in 30:70 stoichiometric ratio.
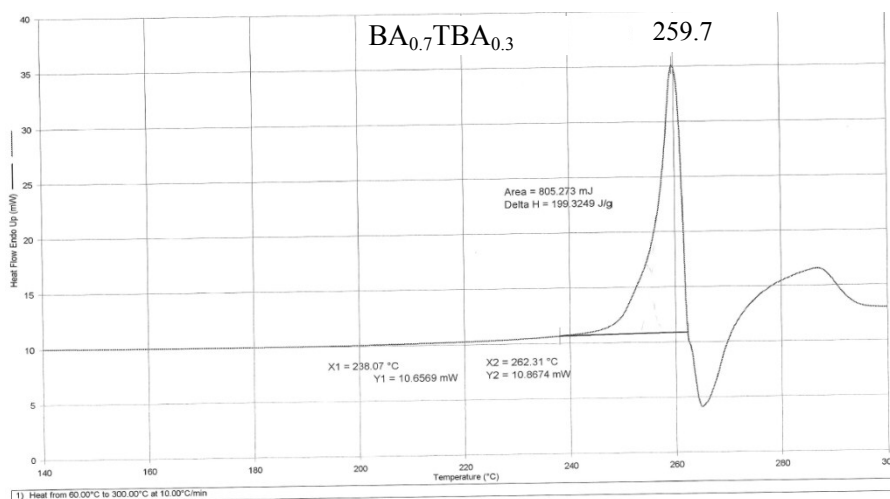

DSC trace of the product of crystallization of BA form II and TBA form I in 40:60 stoichiometric ratio.
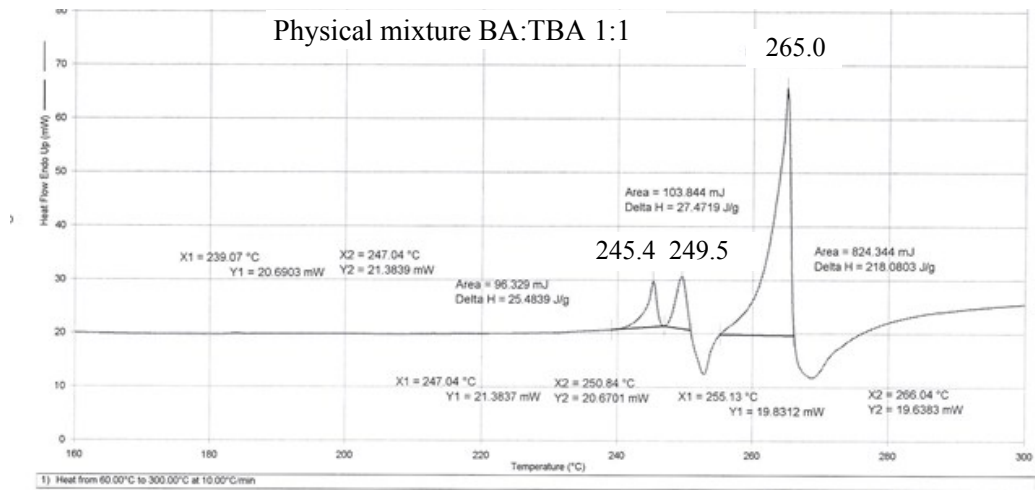
DSC trace of the product of crystallization of BA form II and TBA form I in 50:50 stoichiometric ratio.

DSC trace of the product of crystallization of BA form II and TBA form I in 60:40 stoichiometric ratio.

DSC trace of the product of crystallization of BA form II and TBA form I in 70:30 stoichiometric ratio.

DSC of a 1:1 physical mixture of BA form II and TBA I, showing formation of the $BA_{0.5}TBA_{0.5}$ co-crystal upon melting of the two components.